



HAL
open science

Understanding the contrasting North Atlantic Oscillation anomalies of the winters of 2010 and 2014

Gwendal Rivière, Marie Drouard

► **To cite this version:**

Gwendal Rivière, Marie Drouard. Understanding the contrasting North Atlantic Oscillation anomalies of the winters of 2010 and 2014. *Geophysical Research Letters*, 2015, 42, pp.6868-6875. 10.1002/2015GL065493 . hal-04114761

HAL Id: hal-04114761

<https://hal.science/hal-04114761>

Submitted on 5 Jun 2023

HAL is a multi-disciplinary open access archive for the deposit and dissemination of scientific research documents, whether they are published or not. The documents may come from teaching and research institutions in France or abroad, or from public or private research centers.

L'archive ouverte pluridisciplinaire **HAL**, est destinée au dépôt et à la diffusion de documents scientifiques de niveau recherche, publiés ou non, émanant des établissements d'enseignement et de recherche français ou étrangers, des laboratoires publics ou privés.

Copyright

RESEARCH LETTER

10.1002/2015GL065493

Key Points:

- The North Atlantic Oscillation phases of 2010 and 2014 come from North Pacific anomalies
- Synoptic waves form the cornerstone of the link between North Pacific and North Atlantic anomalies
- Synoptic Rossby waves are shown to trigger new low-frequency atmospheric anomalies

Correspondence to:

G. Rivière,
grieviere@lmd.ens.fr

Citation:

Rivière, G., and M. Drouard (2015), Understanding the contrasting North Atlantic Oscillation anomalies of the winters of 2010 and 2014, *Geophys. Res. Lett.*, *42*, 6868–6875, doi:10.1002/2015GL065493.

Received 22 JUL 2015

Accepted 12 AUG 2015

Accepted article online 21 AUG 2015

Published online 28 AUG 2015

Understanding the contrasting North Atlantic Oscillation anomalies of the winters of 2010 and 2014

Gwendal Rivière¹ and Marie Drouard²

¹Laboratoire de Météorologie Dynamique/IPSL, ENS, CNRS, Paris, France, ²CNRM-GAME, Météo-France and CNRS, Toulouse, France

Abstract The present study investigates the two contrasting winters of 2010 and 2014 during which the North Atlantic Oscillation (NAO) was mainly negative and positive, respectively. In the North Pacific, contrasting anomalies were also present, with a straight zonal Pacific jet in 2010 and a strong poleward deviation of the Pacific jet in its exit region in 2014. Using reanalysis data sets and adopting a nonlinear initial-value approach with a quasi-geostrophic model, we show that the Pacific-North American anomalies are responsible for shaping synoptic wave trains propagating across North America. This in turn largely determines the nature of wave breaking and the synoptic eddy feedback onto the mean flow in the North Atlantic and finally the NAO phase. In such a proposed mechanism, synoptic wave activity forms the cornerstone of the dynamical relationship between the North Pacific and North Atlantic large-scale anomalies during the contrasting winters of 2010 and 2014.

1. Introduction

Recent boreal winters exhibited extreme opposite phases of the North Atlantic Oscillation (NAO). The winter of 2009/2010 (hereafter referred to as 2010) was marked by a strong negative NAO leading to extreme cold episodes over Europe [Ouzeau *et al.*, 2011; Harnik *et al.*, 2014]. On the contrary, the winters of 2011/2012 and 2013/2014 (hereafter referred to as 2012 and 2014, respectively) were dominated by positive NAO, with many strong storms hitting northwestern Europe in 2014 [Santos *et al.*, 2013; Kendon and McCarthy, 2015]. The North Pacific also experienced very different circulations during these winters. Because of a strong El Niño year in 2010, the Pacific jet was anomalously zonal and equatorward shifted [Li and Lau, 2012; Harnik *et al.*, 2014]. On the contrary, the winters of 2012 and 2014 were both characterized by an anomalous large-scale ridge in the Gulf of Alaska. In 2012, the ridge emerges as the response to a La Niña event [Santos *et al.*, 2013; Seager *et al.*, 2014], while in 2014 the ridge is found to originate from warm sea surface temperature anomalies in the tropical western Pacific [Wang *et al.*, 2014; Seager *et al.*, 2014; Hartmann, 2015]. Note that the coexistence of a trough (ridge) anomaly in the northeast Pacific and a negative (positive) NAO phase is typical of a negative (positive) Northern Annular Mode/Arctic Oscillation (NAM/AO) phase [Thompson and Wallace, 2000].

The linkage between North Pacific and North Atlantic low-frequency atmospheric anomalies are often described in terms of quasi-stationary-propagating Rossby waves in the troposphere [Jin and Hoskins, 1995; Honda *et al.*, 2001]. Another potential pathway between the two regions is via the stratosphere [Castanheira and Graf, 2003]. A more recent view has been provided in terms of synoptic waves propagating from the North Pacific storm track to the North Atlantic storm track [Li and Lau, 2012; Drouard *et al.*, 2013]. More precisely, using a three-level quasi-geostrophic model, Drouard *et al.* [2013, hereafter denoted as DRA13] showed that a ridge anomaly in the eastern Pacific, which induces a poleward deflection of the Pacific jet in its exit region, affects the propagation of synoptic waves in such a way that they anomalously propagate equatorward downstream of the ridge over North America. This leads to anticyclonic Rossby wave breakings in the North Atlantic that push the Atlantic jet poleward and trigger the positive NAO. In contrast, a trough anomaly in the eastern Pacific induces a more zonal orientation and a more equatorward position of the Pacific jet than usual. In such large-scale conditions, synoptic waves zonally propagate over North America, which is more likely to induce more cyclonic wave-breaking events than usual in the North Atlantic and the negative NAO. Drouard *et al.* [2015, hereafter denoted as DRA15] have shown some subtle ramifications of the previous mechanism and how it may provide a dynamical interpretation for the existence of the NAM. Note that there are also other studies that have investigated the role played by synoptic waves coming from the Pacific in triggering the NAO [Franzke *et al.*, 2004; Rivière and Orlanski, 2007; Strong and Magnusdottir, 2008; Li and Lau, 2012].

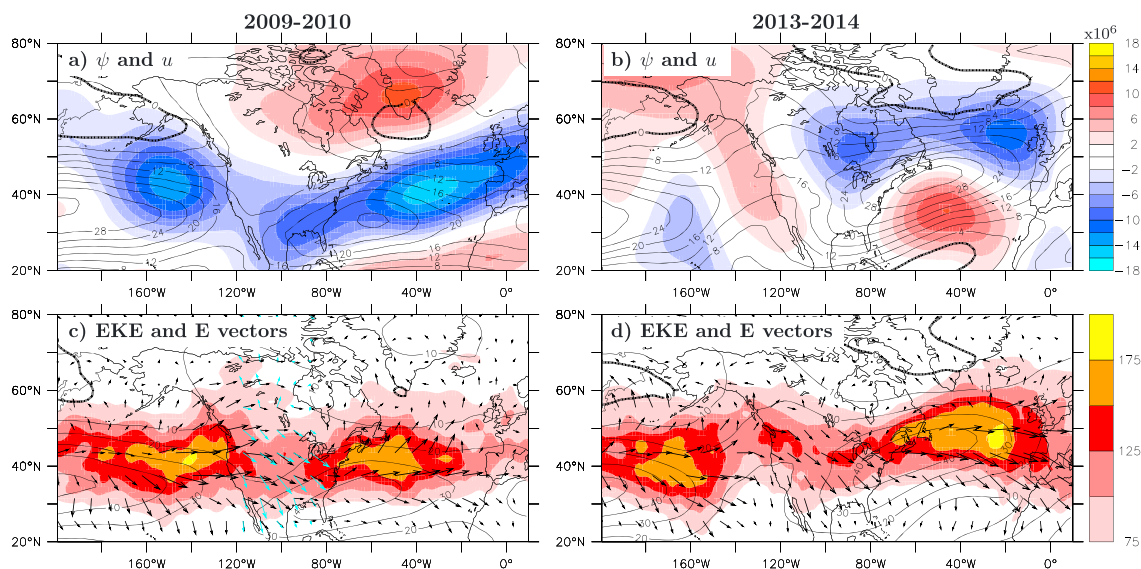


Figure 1. (a, b) Stream function anomalies (shadings; units: $m^2 s^{-1}$) and zonal wind at 500 hPa (contours; interval $4 m s^{-1}$). (c, d) High-frequency eddy kinetic energy (shadings; units: $m^2 s^{-2}$), zonal wind (contours; interval $10 m s^{-1}$) and **E** vectors at 300 hPa (black arrows; units: $m^2 s^{-2}$). (left) The 2009–2010 and (right) 2013–2014 winters. In Figure 1c, the blue arrows correspond to the same **E** vectors shown in black in Figure 1d over North America.

The main goal of the present study is to show that the NAO anomalies of the 2010 and 2014 winters can be solely formed by the DRA13 mechanism, that is, by synoptic Rossby wave-breaking events whose nature is largely determined by the large-scale North Pacific–North American anomalies of the respective winters. While the mechanism was already shown to be active in reanalysis data sets by DRA15, there is always an ambiguity when using reanalysis data sets about the relative importance of other processes. So the main originality of the present paper is to adopt a numerical approach which discards all the other competitive processes (stratospheric control, quasi-stationary propagating Rossby waves) and keeps the key ingredients of the tested mechanism only.

2. Analysis of the Contrasting Winters Using ERA-Interim Data Set

We use daily means of ERA-Interim reanalysis field data sets [Dee *et al.*, 2011] from the European Center for Medium-Range Weather Forecast (ECMWF) on a $1.5^\circ \times 1.5^\circ$ grid from December to March. The anomalous field of each winter is obtained by removing the seasonal climatological cycle. A high-pass filter with a 10 day period is used to have some insight on storm track eddy activity.

The anomalous stream function of the winter of 2010 exhibits the typical dipolar anomaly of the negative NAO and a large-scale trough anomaly in the eastern Pacific (Figure 1a). These anomalies correspond to a more zonal orientation and a more equatorward position of the Pacific and Atlantic jets. On the contrary, the winter of 2014 presents a more positive NAO-like pattern in the North Atlantic, a large-scale trough anomaly centered over eastern Canada, and a large-scale ridge anomaly extending from Alaska to subtropics along the western coast of North America (Figure 1b). The latter two anomalies create a strong northerly flow over North America, bringing cold Arctic air into central North America and creating very unusual cold conditions there [Wang *et al.*, 2014; Hartmann, 2015]. Hence, there is a strong poleward deflection of the Pacific jet in its exit region and a southwest-northeast tilted Atlantic jet, which is well separated from the African subtropical jet as typical during positive NAO.

The high-frequency eddy kinetic energy (EKE) and the so-called **E** vectors [Trenberth, 1986; Rivière *et al.*, 2003] are shown in Figures 1c and 1d. In the North Pacific, there is not much difference in the amount of EKE between the two winters. The spatial distribution of EKE is different with a Pacific storm track extending farther east in 2010 compared to 2014. Over North America, no difference in EKE can be noticed suggesting that downstream development (i.e., the amount of downstream propagation of synoptic wave energy [Chang, 1993]) is similar in 2010 and 2014. However, the **E** vectors of the two winters exhibit different orientations over North America (compare the blue and black arrows in Figure 1c). In 2010, the **E** vectors are mainly eastward oriented, suggesting a zonal propagation of synoptic waves. In 2014, the **E** vectors are southeastward oriented downstream of

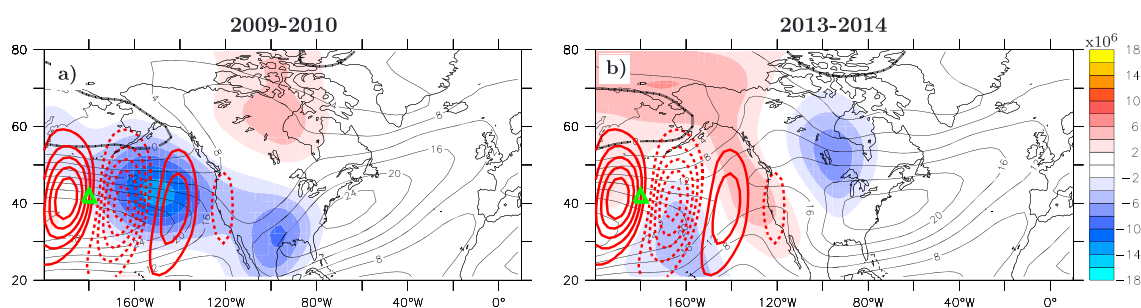


Figure 2. (a, b) Basic-state stream function anomalies relative to the climatology from the North Pacific to 100°W (shadings; units: $m^2 s^{-1}$) and basic-state zonal wind at 500 hPa (contours; interval $4 m s^{-1}$) for the 2009–2010 and 2013–2014 cases, respectively. The initial perturbation meridional wind at 500 hPa centered at 180°W, 42°N (green triangle) is shown in red contours (dashed and solid contours for negative and positive values, respectively; interval: $4 m s^{-1}$).

the ridge anomaly suggesting that the waves start propagating equatorward from that region. It confirms the effect of a large-scale ridge anomaly on synoptic wave propagation analyzed in DRA13. In the North Atlantic, EKE is stronger and extends much more northeastward in 2014 than in 2010, consistent with the contrasting NAO phases. The **E** vectors have mainly poleward and equatorward orientation during 2010 and 2014, respectively, which reflects the dominance of cyclonic and anticyclonic wave-breaking events during negative and positive NAO [Benedict et al., 2004; Rivière and Orlanski, 2007].

3. Model and Setup of the Numerical Experiments

We use the three-level quasi-geostrophic model on the sphere of Marshall and Molteni [1993] which integrates the following potential vorticity (PV) equation at each vertical level i :

$$\frac{\partial q_i}{\partial t} = -J(\psi_i, q_i) - D_i(\psi_1, \psi_2, \psi_3) + J(\bar{\psi}_i, \bar{q}_i) + D_i(\bar{\psi}_1, \bar{\psi}_2, \bar{\psi}_3), \quad (1)$$

where q_i and ψ_i denote the PV and stream function, respectively. Each variable is the sum of a perturbation and a basic flow denoted with primes and bars, respectively ($q_i = \bar{q}_i + q'_i$, $\psi_i = \bar{\psi}_i + \psi'_i$). Levels 1–3 correspond to 200, 500, and 800 hPa, respectively. J denotes the Jacobian and D_i a dissipation term including a Newtonian cooling in temperature, a low-level Ekman dissipation, and a diffusion term. The topography is included through the formulation of the PV and dissipation term at the lowest level. The parameters are set as in DRA13 and a T42 truncation is used.

In the North Pacific and over North America (200°W–100°W; 20°N–80°N), the basic flow is composed of the winter climatological flow plus the large-scale anomalies of each individual winter (i.e., one of those shown in Figure 1). Elsewhere and, in particular, in the North Atlantic, the basic flow is only composed of the climatological flow. A smooth mask with the use of a Gaussian function is applied outside the Pacific-North American domain so that the large-scale anomalies smoothly decrease to zero outside the domain. The results of this mask is shown by comparing Figure 2a with Figure 1a and Figure 2b with Figure 1b. Therefore, the two basic flows shown in Figure 2 (black contours) only differ in the Pacific-North American sector, where they correspond to the contrasting averaged circulations of the 2010 and 2014 winters. In the Atlantic sector, east of 80°W, the two basic flows are identical.

At the initial time the flow is composed of the sum of the basic flow and a synoptic-scale disturbance. The latter is defined by regressing the high-pass stream function against the high-pass stream function at a particular base point inside the Pacific storm track. The initial disturbance is 4 times the regression to initialize the model with a realistic-amplitude wave (around $40 m^{-1}$ for the 200 hPa perturbation meridional wind). An example of such a perturbation is shown in Figure 2 for a base point located at 180°W, 42°N. The idea is to introduce a synoptic-scale wave train slightly upstream of the large-scale anomalies of the Pacific-North American sector, to let it propagate through these anomalies and investigate its impact in the Atlantic sector.

The forcing terms (i.e., the two last terms on the right-hand side (RHS) of equation (1)) are such that the basic flow is maintained stationary with time. The purpose of such a forcing is to prevent the large-scale anomalies from propagating downstream and to be sure that the flow modification in the Atlantic sector is solely due to the synoptic wave train. The setup of the numerical experiments is similar to section 4 of DRA13. However,

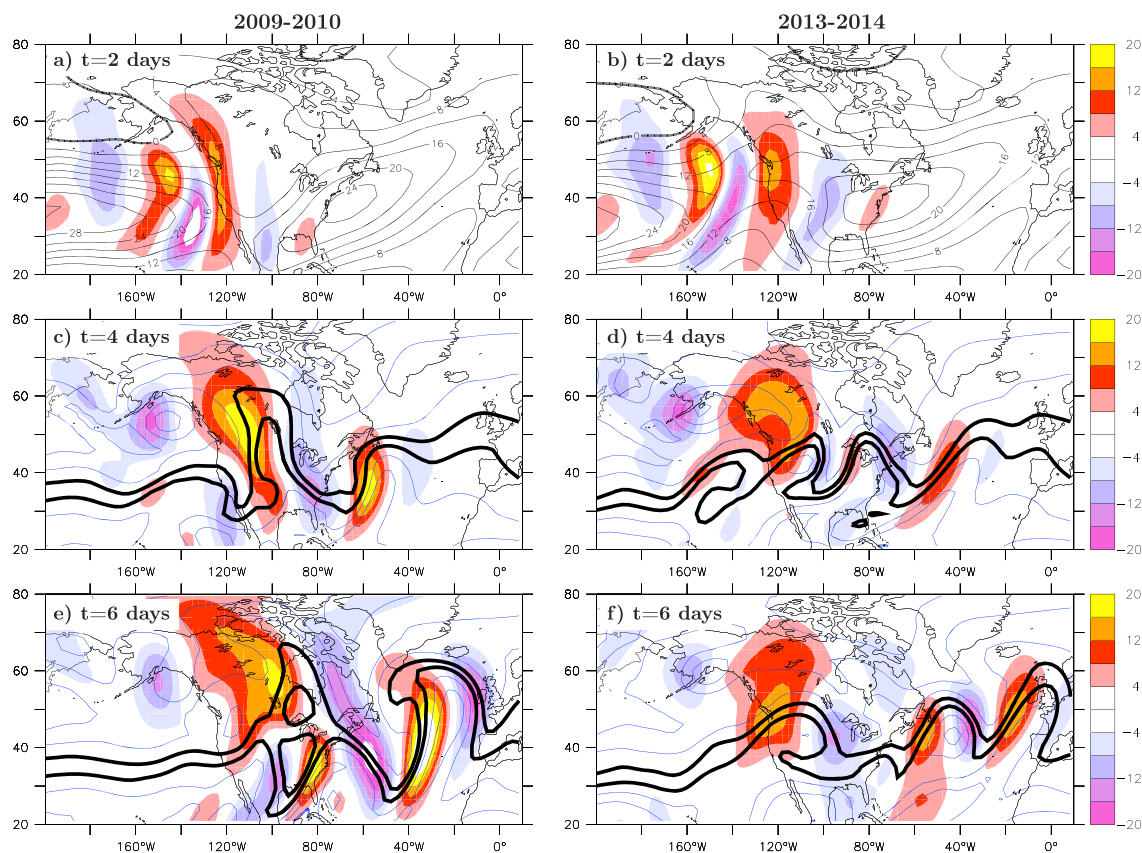


Figure 3. Time evolution of the 500 hPa perturbation meridional wind (shadings; units: m s^{-1}) for (a, c, and e) the 2009–2010 case and (b, d, and f) the 2013–2014 case. In Figures 3a and 3b, the black contours correspond to the 500 hPa basic-state zonal wind (interval: 4 m s^{-1}). In Figures 3c–3f, the contours represent the 500 hPa potential vorticity (interval: $4 \times 10^{-5} \text{ s}^{-1}$) with black contours corresponding to the 1.2 and $1.6 \times 10^{-4} \text{ s}^{-1}$ values.

we here consider real anomalies whereas in DRA13 they were artificially built up. Furthermore, additional sensitivity experiments are also performed which were not considered in DRA13.

4. Results of the Numerical Experiments

Figure 3 shows the time evolution of the simulation initialized with the synoptic disturbance centered at 180°W , 42°N shown in Figure 2. At $t = 2$ days, the synoptic wave packet propagates across the eastern Pacific and North America. Since the westerly jet is more equatorward (poleward) located for the 2010 (2014) case, the waves propagate more equatorward (poleward). Note, in particular, the more southern route of synoptic eddies over North America which is a systematic feature of El Niño events [Seager *et al.*, 2010; Basu *et al.*, 2013]. Eddies’ tilts located upstream of the wave packet envelope (i.e., west of 140°W) are mostly the same for the two cases, but they significantly differ more downstream. Over North America, the eddies are meridionally tilted for the 2010 case whereas they are anticyclonically tilted for the 2014 case. Such a difference increases with time. At $t = 4$ days, for the 2010 case (Figure 3c), the cyclonic tilt dominates over North America leading to a major cyclonic wave-breaking event characterized by cyclonic overturnings of the PV contours. In the same region, for the 2014 case (Figure 3d), two anticyclonic wave-breaking events (i.e., two regions of anticyclonic overturnings of PV contours) appear, one at 140°W and another at 100°W . Even though there are no wave-breaking events in the Atlantic sector at $t = 4$ days, differences in eddies’ tilts between the two cases are already visible there. At $t = 6$ days, a major cyclonic wave-breaking event occurs in the mid-Atlantic for the 2010 case (Figure 3e) and two anticyclonic wave-breaking events of smaller amplitude appear in the Atlantic sector for the 2014 case, with the stronger one being over Western Europe (Figure 3f).

The cyclonic and anticyclonic tilt of the waves during their breaking correspond to equatorward and poleward eddy momentum fluxes, respectively. As such, during cyclonic wave breaking there is a deposit of westward momentum on the poleward flank of the jet and eastward momentum in the jet core and on the equa-

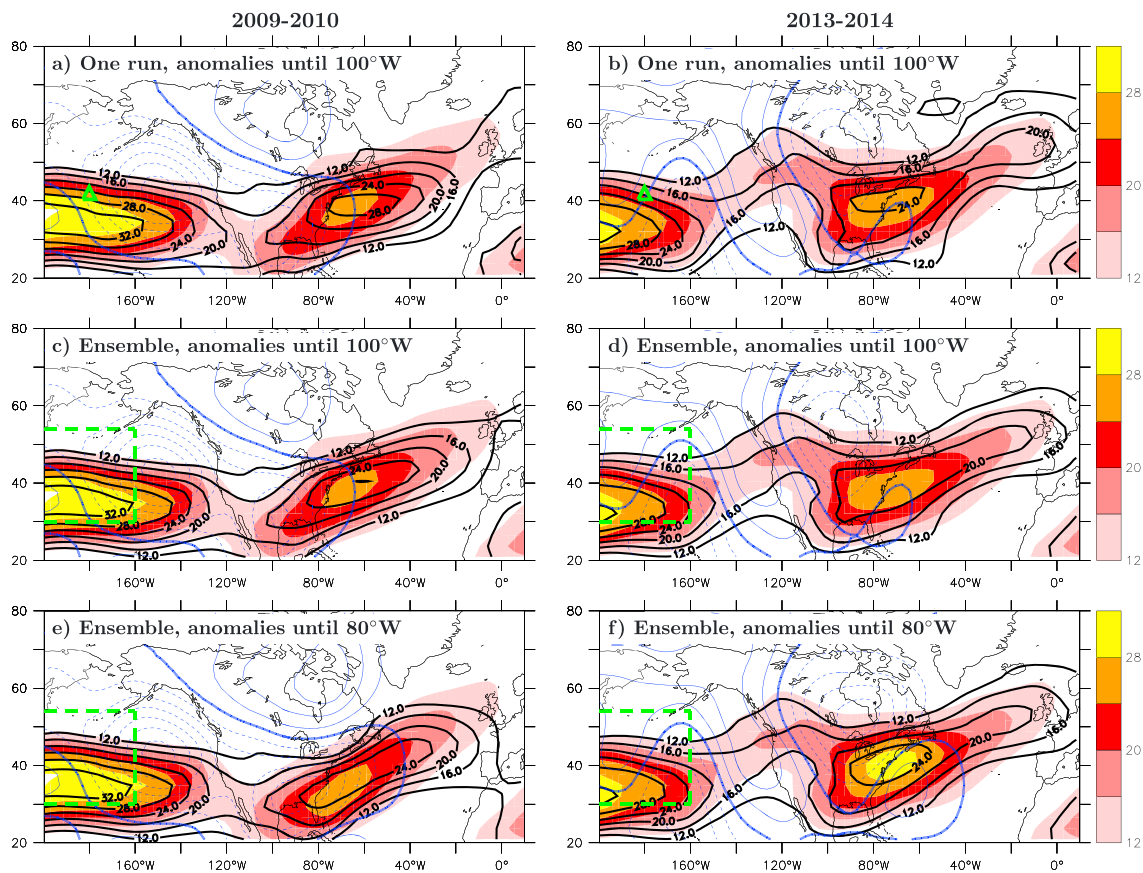


Figure 4. Zonal wind averaged between $t = 8$ days and $t = 14$ days (black contours; interval: 4 m s^{-1} for values greater than 12 m s^{-1}), basic-state zonal wind (shadings; units: m s^{-1}) and basic-state stream function anomalies at 500 hPa (blue contours; interval: $2 \times 10^6 \text{ m}^2 \text{ s}^{-1}$). (a, b) correspond to one simulation with an initial perturbation centered at 180°W , 42°N (green triangle). (c–f) Ensemble means of 81 simulations with initial perturbations centered over a grid point inside the green box. In Figures 4a–4d the basic-state stream function anomalies extend to 100°W and in Figures 4e and 4f they extend to 80°W . Left and right columns correspond to the 2009–2010 and 2013–2014 winters, respectively.

toward flank. The converse occurs for anticyclonic wave breaking. This general picture may fluctuate from case to case depending on the position of the breaking event relative to the mean jet. But generally speaking, eddy momentum flux convergence anomalies associated with anticyclonic and cyclonic wave-breaking events induce poleward and equatorward shifts of the jet, respectively [Rivière and Orlanski, 2007; Vallis and Gerber, 2008]. Alternative arguments to explain the dynamical link between wave breaking and the NAO are provided in Benedict et al. [2004].

Figure 4 shows the mean flow modification after the migration of the synoptic wave and its breaking in the North Atlantic, which occurs mainly after 1 week. The cyclonic and anticyclonic wave-breaking events of the 2010 and 2014 runs are accompanied by an equatorward and a poleward shifted Atlantic jet, consistent with the reasoning of the previous paragraph (Figures 4a and 4b). Furthermore, the jet is more zonal for the 2010 case and more southwest-northeast tilted for the 2014 case, similarly to the negative and positive NAO, respectively. The result is robust when considering an ensemble mean of simulations initialized with disturbances centered at different location within the Pacific storm track (Figures 4c and 4d). The ensemble mean for the 2014 case shows a northeastward acceleration of the Atlantic jet while that of the 2010 case shows a southward—albeit limited—shift of the jet.

To further investigate if the western Atlantic baroclinicity can influence the downstream part of the Atlantic jet, additional experiments were made by extending the anomalies farther east. In Figures 4e and 4f the mask was applied west of 80°W allowing the basic flow to be modified in the western Atlantic until 60°W . Such an extension leads to a more southward and weaker basic jet maximum for the 2010 case than for the 2014 case (compare the shadings in Figures 4e and 4f in the longitudinal band 80°W – 60°W). For the 2014 case, the Atlantic eddy-driven jet is not impacted by the eastward extension of the large-scale anomalies (the contours

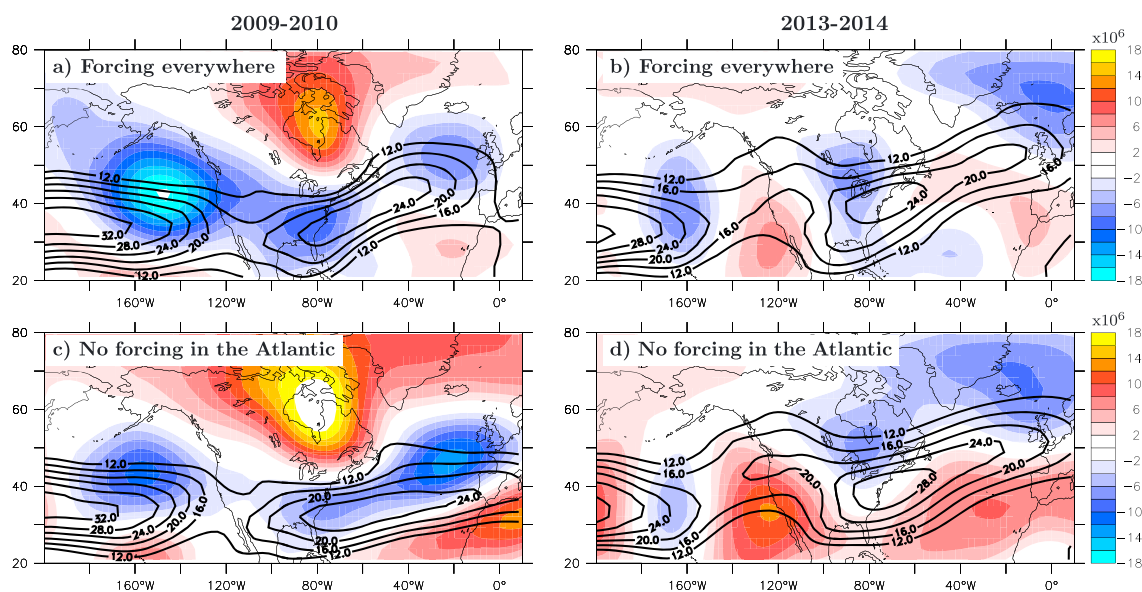


Figure 5. Stream function anomalies (shadings; units: $\text{m}^2 \text{s}^{-1}$) and zonal wind at 500 hPa (contours; interval: 4 m s^{-1} for values greater than 12 m s^{-1}) averaged between $t = 8$ days and 14 days. (a, b) The same ensemble mean shown in Figures 4e and 4f, respectively. (c, d) Same as Figures 5a and 5b, respectively, except that the forcing is set to a spatially homogeneous constant by spatially averaging the forcing terms on the RHS of equation (1) in the Atlantic sector ($60^\circ\text{W} - 0^\circ\text{W}$; $20^\circ\text{N} - 60^\circ\text{N}$). Left and right columns correspond to the 2009–2010 and 2013–2014 winters, respectively.

of Figures 4d and 4f are similar). However, for the 2010 case, the Atlantic jet is located farther south between 40°W and 10°E and is now connected to the African subtropical jet when the baroclinicity has been modified at the entrance of the Atlantic domain (compare the contours of Figures 4c and 4e). It is consistent with Rivière [2009] showing that a more southward baroclinicity at the entrance of a storm track favors more cyclonic wave breaking farther downstream and a more southward shifted jet at the end of the storm track. Therefore, differences between the 2010 and 2014 cases amplify when the western Atlantic baroclinicity is modified.

The jet obtained in the previous 2010 runs is not really zonal, and the large-scale anomalies obtained in the Atlantic sector do not correspond to a negative NAO pattern as the anticyclonic anomaly over Greenland is rather weak and the cyclonic anomaly is located too far north (compare Figure 5a with Figure 1a). The positive NAO pattern of Figure 5b is clearer even though the anomalies are not located at the same place as in 2014. One may argue that the forcing in the Atlantic sector which tends to restore the climatological flow prevents strong latitudinal fluctuations of the Atlantic jet. To further investigate this hypothesis, simulations were performed by reducing the forcing terms on the RHS of equation (1) in the Atlantic sector to a spatially homogeneous constant. More precisely, the forcing term is replaced by its spatial average over the domain ($60^\circ\text{W} - 0^\circ\text{W}$; $20^\circ\text{N} - 60^\circ\text{N}$) to suppress any restoration of the climatological flow there. However, the initial flow is still the climatological flow in that sector. For such runs, much larger fluctuations of the Atlantic jet and much stronger stream function anomalies are obtained. In particular, there is the formation of strongly negative and positive NAO phases for the 2010 and 2014 cases, respectively (Figures 5c and 5d). Therefore, from the sole knowledge of the large-scale anomalies in the Pacific–North American sector, we successfully reproduced extreme NAO phases, similarly to what happened during the two contrasting winters (compare the shadings of Figures 5c and 5d with Figures 1a and 1b).

5. Conclusion

The present study aimed at showing that synoptic eddy activity have probably played a key role in the formation and maintenance of the NAO anomalies during the contrasting winters of 2010 and 2014. Our view is that the large-scale anomalies in the North Pacific and over North America, which originate from sea surface temperature anomalies in the tropical Pacific [Wang et al., 2014; Seager et al., 2014; Hartmann, 2015], are responsible for the shaping of synoptic wave trains propagation across North America. This in turn largely determines the nature of wave breaking, the synoptic eddy feedback onto the mean flow in the North Atlantic and thus the NAO phase. Such a view was first confirmed using reanalysis data sets by showing the difference

in wave propagation and horizontal tilts over North America. This was further demonstrated by adopting a nonlinear initial-value problem using a quasi-geostrophic model. Finite-amplitude synoptic disturbances are initialized in the North Pacific upstream of the large-scale Pacific–North American anomalies of interest. The short-term simulations show the propagation of the synoptic waves across North America, their breaking in the North Atlantic, and finally their feedback onto the Atlantic jet. For the 2014 case, the presence of a ridge anomaly in the northeastern Pacific creates a strong deviation of the Pacific jet. This induces an equatorward propagation of the synoptic wave trains in the North Atlantic and so more anticyclonic breaking, together with a poleward shifted Atlantic jet. On the contrary, for the 2010 case, the presence of the zonally oriented Pacific jet favors a more zonal propagation of the wave trains, a more meridional elongation of the disturbances. This leads to more cyclonic wave breaking than usual in the Atlantic and an equatorward displacement of the Atlantic jet. As such, the contrasting NAO phases of 2010 and 2014 can be reproduced from the sole knowledge of the Pacific–North American anomalies of the considered winters and keeping the effect of synoptic waves only.

The setup of our numerical approach discarded the influence of the stratosphere and the quasi-stationary Rossby waves on purpose. Indeed, our objective was to adopt a strategy to test the ability of synoptic waves to form NAO-like anomalies. The proposed mechanism is not exclusive. The stratosphere may have played a role during the winter of 2010 as suggested by *Ouzeau et al.* [2011]. For instance, a major sudden stratospheric warming occurred in late January [Dörnbrack et al., 2012] just before an abrupt decrease in the NAO index (not shown), suggesting a possible downward propagation of NAM anomalies [Baldwin and Dunkerton, 1999]. The downstream propagation of quasi-stationary Rossby waves was shown to explain the ridge trough anomaly of 2014 in the Pacific–North American sector by *Wang et al.* [2014], but such a paradigm was not invoked to explain the NAO anomalies. Future studies would be necessary to investigate the likelihood of these competitive processes.

Acknowledgments

The ERA-Interim data were obtained at <http://apps.ecmwf.int/datasets/data/interim-full-daily/>.

The Editor thanks two anonymous reviewers for their assistance in evaluating this paper.

References

- Baldwin, M. P., and T. J. Dunkerton (1999), Propagation of the Arctic Oscillation from the stratosphere to the troposphere, *J. Geophys. Res.*, *104*, 30,937–30,946.
- Basu, S., X. Zhang, I. Polyakov, and U. S. Bhatt (2013), North American winter-spring storms: Modeling investigation on tropical Pacific sea surface temperature impacts, *Geophys. Res. Lett.*, *40*, 5228–5233, doi:10.1002/grl.50990.
- Benedict, J. J., S. Lee, and S. B. Feldstein (2004), Synoptic view of the North Atlantic Oscillation, *J. Atmos. Sci.*, *61*, 121–144.
- Castanheira, J., and H.-F. Graf (2003), North Pacific–North Atlantic relationships under stratospheric control, *J. Geophys. Res.*, *108*(D1), 4036, doi:10.1029/2002JD002754.
- Chang, E. K. M. (1993), Downstream development of baroclinic waves as inferred from regression analysis, *J. Atmos. Sci.*, *50*, 2038–2053.
- Dee, D. P., et al. (2011), The ERA-Interim reanalysis: Configuration and performance of the data assimilation system, *Q. J. R. Meteorol. Soc.*, *137*, 553–597.
- Dörnbrack, A., M. C. Pitts, L. R. Poole, Y. J. Orsolini, K. Nishii, and H. Nakamura (2012), The 2009–2010 Arctic stratospheric winter—general evolution, mountain waves and predictability of an operational weather forecast model, *Atmos. Chem. Phys.*, *12*, 3659–3675.
- Drouard, M., G. Rivière, and P. Arbogast (2013), The North Atlantic Oscillation response to large-scale atmospheric anomalies in the northeastern Pacific, *J. Atmos. Sci.*, *70*, 2854–2874.
- Drouard, M., G. Rivière, and P. Arbogast (2015), The link between the North Pacific climate variability and the North Atlantic Oscillation via downstream propagation of synoptic waves, *J. Clim.*, *28*, 3957–3976.
- Franzke, C., S. B. Feldstein, and S. Lee (2004), Is the North Atlantic Oscillation a breaking wave?, *J. Atmos. Sci.*, *61*, 145–160.
- Harnik, N., E. Galanti, O. Martius, and O. Adam (2014), The anomalous merging of the African and North Atlantic jet streams during the Northern Hemisphere winter of 2010, *J. Clim.*, *27*, 7319–7334.
- Hartmann, D. L. (2015), Pacific sea surface temperature and the winter of 2014, *Geophys. Res. Lett.*, *42*, 1894–1902, doi:10.1002/2015GL063083.
- Honda, M., H. Nakamura, J. Ukita, I. Kousaka, and K. Takeuchi (2001), Interannual seesaw between the Aleutian and Icelandic lows. Part I: Seasonal dependence and life cycle, *J. Clim.*, *14*, 1029–1042.
- Jin, F., and B. J. Hoskins (1995), The direct response to tropical heating in a baroclinic atmosphere, *J. Atmos. Sci.*, *52*, 307–319.
- Kendon, M., and M. McCarthy (2015), The UK's wet and stormy winter of 2013/2014, *Weather*, *70*, 40–47.
- Li, Y., and N.-C. Lau (2012), Contributions of downstream eddy development to the teleconnection between ENSO and the atmospheric circulation over the North Atlantic, *J. Clim.*, *25*, 4993–5010.
- Marshall, J., and F. Molteni (1993), Toward a dynamical understanding of planetary-scale flow regimes, *J. Atmos. Sci.*, *50*, 1792–1818.
- Ouzeau, G., J. Cattiaux, H. Douville, A. Ribes, and D. Saint-Martin (2011), European cold winter 2009–2010: How unusual in the instrumental record and how reproducible in the ARPEGE-climat model?, *Geophys. Res. Lett.*, *38*, L11706, doi:10.1029/2011GL047667.
- Rivière, G. (2009), Effect of latitudinal variations in low-level baroclinicity on eddy life cycles and upper-tropospheric wave-breaking processes, *J. Atmos. Sci.*, *66*, 1569–1592.
- Rivière, G., and I. Orlanski (2007), Characteristics of the Atlantic storm-track eddy activity and its relation with the North Atlantic Oscillation, *J. Atmos. Sci.*, *64*, 241–266.
- Rivière, G., B. Hua, and P. Klein (2003), Perturbation growth in terms of barotropic alignment properties, *Q. J. R. Meteorol. Soc.*, *129*, 2613–2635.
- Santos, J. A., T. Woollings, and J. G. Pinto (2013), Are the winters 2010 and 2012 archetypes exhibiting extreme opposite behavior of the North Atlantic jet stream?, *Mon. Weather Rev.*, *141*, 3626–3640.

- Seager, R., N. Naik, M. Ting, M. Cane, N. Harnik, and Y. Kushnir (2010), Adjustment of the atmospheric circulation to tropical Pacific SST anomalies: Variability of transient eddy propagation in the Pacific-North America sector, *Q. J. R. Meteorol. Soc.*, *136*, 277–296.
- Seager, R., M. Hoerling, S. Schubert, H. Wang, B. Lyon, A. Kumar, J. Nakamura, and H. Henderson (2014), Causes and predictability of the 2011–2014 California drought, *Rep.*, *40*, doi:10.7289/V7258K7771F.
- Strong, C., and G. Magnúsdóttir (2008), How Rossby wave breaking over the Pacific forces the North Atlantic Oscillation, *Geophys. Res. Lett.*, *35*, L10706, doi:10.1029/2008GL033578.
- Thompson, D. W. J., and J. M. Wallace (2000), Annular modes in the extratropical circulation. Part 1: Month-to-month variability, *J. Clim.*, *13*, 1000–1016.
- Trenberth, K. (1986), An assessment of the impact of transient eddies on the zonal flow during a blocking episode using localized Eliassen-Palm flux diagnostics, *J. Atmos. Sci.*, *43*, 2070–2087.
- Vallis, G., and E. Gerber (2008), Local and hemispheric dynamics of the North Atlantic Oscillation, annular patterns and the zonal index, *Dyn. Atmos. Oceans*, *44*, 184–212.
- Wang, S.-Y., L. Hipps, R. R. Gillies, and J.-H. Yoon (2014), Probable causes of the abnormal ridge accompanying the 2013–2014 California drought: ENSO precursor and anthropogenic warming footprint, *Geophys. Res. Lett.*, *41*, 3220–3226, doi:10.1002/2014GL059748.